

Design and Analysis of Ultra-wideband and High Directive THz Photoconductive Vivaldi Antenna

Jawad Yousaf^{1,2}, Amira Dhiflaoui³, Ali Yahyaoui^{3,4}, Bandar Hakim¹, Mohamed Zarouan¹, Wassim Zouch¹, Taoufik Aguil³, and Hatem Rmili¹

¹Electrical and Computer Engineering Department, Faculty of Engineering, King Abdulaziz University
P.O. Box 80204, Jeddah 21589, Saudi Arabia
hmrili@kau.edu.sa

²Department of Electrical and Computer Engineering, Abu Dhabi University, United Arab Emirates

³University of Tunis El Manar (UTM), National Engineering School of Tunis (ENIT)
Communications Systems Laboratory (SysCom), BP 37, Belvédère 1002 Tunis, Tunisia

⁴Electrical and Electronic Engineering Department, College of Engineering, University of Jeddah
P.O. Box 80327, Jeddah 21589, Saudi Arabia

Abstract – In this work a novel design of an ultra-wideband and highly directive Vivaldi photoconductive antenna (PCA) is reported for the first time for the THz sensing and imaging applications. The optical-to-THz conversion efficiency for the enhanced directivity of the reported PCA is enhanced by adding a hemispherical silicon-based lens with the PCA gold electrode and quartz substrate ($\epsilon_r = 3.78$, $\tan \delta = 0.0001$). The optimization of the antenna design parameters is performed in CST MWS for the frequency range of 1-6 THz. The design antenna has UWB -10 dB impedance and 3-dB AR bandwidths of 6 THz, maximum directivity of 10 dBi and maximum total radiation efficiency of > 40%.

Index Terms – High directivity, log spiral antenna, photoconductive THz antenna, wideband.

I. INTRODUCTION

The frequency band (0.1 to 10 THz) between the infrared and microwave frequencies in the electromagnetic spectrum is referred as the terahertz (THz) band. THz sources have drawn a lot attention recently due to their unique properties of provision high resolution images as compared to the microwave systems and less harm to the human body as compared to the conventionally used X-ray imaging system [1]. Besides imaging systems, the other examples of THz applications includes materials characterizations using spectroscopy [2-4], security screening, high-data rate communication and biomedical analysis [5-9].

The antenna plays a pivot role for the generation of the wideband, narrow beam width, highly directive

and sensitive polarization THz radiations for the aforementioned applications (particular for high resolution imaging system). The photoconduction technique based on the optical-to-terahertz conversion is among the preferred method for the generation of THz waves due to its robust and cheap room temperature operation [1, 10, 11]. Optical to THz conversion efficiency is a key feature for the characterization of the PCAs. It defines the conversion of the input optical photoconductive (lasers) waveforms to the THz waves [12]. Typically, the optical-to-THz efficiency depends on the used photoconductive materials parameters and the employed structure of the PCA [12-15]. The reported examples of the photoconductive antennas (PCAs) for the generation of THz radiations are bow tie [1, 13, 14, 16], dipole planner array [17], Yagi-Uda [18], spiral-shaped [19], and conical horn [10]. Besides the chosen antenna electrodes for the enhanced input infrared radiations (IR) coupling, the selection of antenna substrate material significantly impacts its radiation efficiency [17]. The preferred substrate material for the PCA antennas must have ultra-short lifetime (~ 5- 10 ps) [20, 21], direct band-gap and higher substrate carrier mobility. The common examples of the used substrates in THz community are Si-GaAs [22, 23], LT-GaAs [23-25], and In-GaAs [23, 26].

The directivity of the generated THz waves depends on the optical-to-THz conversion efficiency of the PCA. The authors in [1, 13, 14] reported a bow-tie PCA with a Si-hemispherical lens for the enhanced directivity. Deva *et al.* [10] reported a fixed-frequency conical horn and Si-lens based PCA for the gain enhancement. Gupta *et al.* [13] investigated the effect of the dielectric coating on bow-tie PCA structure for the enhancement of

optical-to-THz conversion efficiency of the designed antenna. Park *et al.* [16] covered the antenna structure with metal nanoislands to form nanoplasmonic PCA for the increase the emission properties of the antenna. In [1, 27], authors combined the PCA with the artificial magnetic conductor (AMC) and metasurface-based flat lens for the enhancement of directivity of the antenna without the need of large sized silicon-based lenses. Malhotra *et al.* [17] combined the planner dipole array with frequency selective surface to enhance the radiation properties of the array PCA. In [28], authors proposed that the utilization of the aspheric lenses can improve the radiation coupling of the PCAs. However, the integration of the metasurface [1, 17, 27] increases the side-lobe levels and front-to-back ratio of the PCAs. Also, the reported designs of [1, 10, 13, 14, 16-19, 27, 28] have limitations of lower impedance bandwidth, AR bandwidth, overall large size of antenna structure and lower directivity.

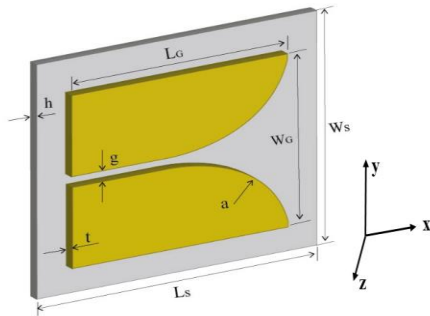


Fig. 1. Schematic of the designed Vivaldi THz antenna without lens; L_S : substrate length, W_S : substrate width, h : substrate thickness, L_G : length of Vivaldi patch, W_G : width of Vivaldi patch, g : minimum width of the tapered slot, a : curvature coefficient, and t : thickness of the Vivaldi patch.

In this work, for the first time, a novel design of ultra-wideband, high directive Vivaldi PCA is proposed. Fig. 1 shows the schematic of the proposed Vivaldi antenna. The Vivaldi patch is made of gold material whereas the quartz ($\epsilon_r = 3.78$, $\tan \delta = 0.0001$) is used as the PCA substrate. The optical-to-terahertz efficiency of the designed antenna is enhanced by integrating a hemispherical silicon-based lens with the PCA electrode (see Fig. 2). The full wave numerical analysis of the designed antenna is performed in CST Microwave Studio (MWS) software in the frequency range of 1 to 6 THz to get the optimal values of Figs. 1 and 2 design parameters. The -10 dB impedance and 3-dB axial ratio (AR) bandwidth of the designed optimized antenna with lens is 6 THz which is the largest among all the reported

legacy designs [1, 10, 13, 14, 16-19, 27, 28] as per our best knowledge.

The rest of the paper is organized as follows. The proposed Vivaldi antenna design procedure is described in Section II. Section III presents the detailed analysis of parametric study of proposed antenna design parameters. The discussion about the optimized antenna results in given in Section IV. Section V describes details the effect of the added lens on the antenna structure on its performance parameters. The comparison of the proposed PCA design with the legacy designs in presented in Section VI. Last Section VII concludes the study.

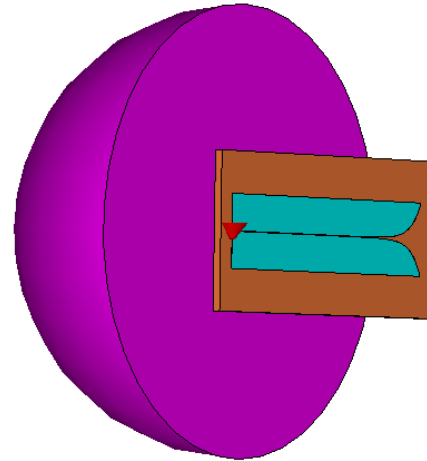


Fig. 2. Designed Vivaldi THz antenna with hemispherical lens having diameter of R_L .

II. ANTENNA DESIGN PROCEDURE

The details of the design of the proposed Vivaldi antenna are described in this section. The initial design of the Vivaldi antenna was reported in 1979 by Gibson [29]. The antenna structure as shown in Fig. 1 constitutes of an exponential curved tapped slot. Besides compact planner structure, the Vivaldi antenna offers additional advantages of high directive, wider impedance bandwidth and linear polarization. The exponential tapered profile of the Fig. 1 antenna slot is obtained using the exponential function of (1):

$$f(x) = A(e^{ax} - e^{-ax}) + \frac{g}{2}, \quad (1)$$

Where

$$A = \frac{g_2 - g}{e^{aL_G} - e^{-a}}. \quad (2)$$

In (1), a defines the curvature coefficient, g and g_2 refer to the minimum and maximum width of the tapered slot respectively, and L_G is the length of antenna patch. Table 1 summarizes the initial design parameters of the proposed ultra-wide band and high directive Vivaldi antenna for the THz range.

Table 1: Vivaldi Antenna design parameters

Parameter	Values (μm)
L_S (Substrate Length)	134
W_S (Substrate width)	60
h (Substrate thickness)	2
L_G (Vivaldi-patch length)	115
W_G (Vivaldi-patch width)	22
g (Minimum width of the tapered slot)	0.3
g_2 (Maximum width of the tapered slot)	22
a (curvature coefficient)	0.5
t (Vivaldi-patch thickness)	0.06

The numerical simulation of the design antenna is performed in CST Microwave Studio (MWS) software. The full wave EM simulation is conducted for the frequency range of 1 to 6 THz. The used substrate in the antenna design in Quartz which have the relative permittivity value of 3.75 and tangent loss value of 0.0001. The Vivaldi patch is made of gold material which is employed for the improvement of the IR radiations. The antenna is fed with the discrete port for the EM simulation in the aforementioned THz frequency range. The full wave numerical simulation of the antenna is performed for the analysis of the antenna impedance, axial ratio, current distribution and radiation characteristics.

After the parametric analysis of the initial design parameters of Table 1 (details in Section III) to get the optimized design values for the UWB impedance and axial ratio (AR) characteristics of the designed PCA, a hemispherical lens is added to the antenna structure to enhance its gain and directivity. Figure 2 shows the schematic of the Vivaldi antenna with the added lens on the backside of the Quartz substrate. The added lens is made of silicon material and has diameter of R_L . The diameter of the lens is varied to obtain the wideband impedance, axial ratio bandwidth and to produce high directivity, high gain and higher total efficiency of the designed antenna.

III. PARAMETRIC STUDY OF UWB THZ VIVALDI ANTENNA

This sections details the parametric analysis of the Table 1 antenna design parameters to obtain the optimal values of those parameters for the desired wideband and high directive antenna characteristics without added lens to the antenna structure. The upper and lower bound of the various antenna design parameters is selected keeping in view the fabrication constrains and also to minimize the memory requirements for the full wave EM analysis of each variant design of the analyzing antenna.

The analysis is performed for the variations in the height of the antenna substrate (h), thickness of the gold conducting Vivaldi patch (t), length (L_G) and width of

Vivaldi (W_G) patch (gold material), curvature exponential variable (a), and minimum width of the antenna slot (g) to find the optimal antenna dimensions for the wideband impedance bandwidth of the designed Vivaldi antenna. Firstly, the optimization analysis of antenna dimensions is conducted without lens for the subsequent study of the antenna performance with lens (details in Section III-B) with the optimal antenna design parameters.

Figure 3 shows the variations in the S_{11} characteristics of the proposed Vivaldi THz antenna when the height (h) of the substrate is varied in the range of 1-4 μm with a step size of 1 μm . The results depict that reflection characteristics of the designed antenna varies with the change in the substrate thickness. The resonance frequencies are shifted back with the increase in the height of the substrate. It can be noted from the Fig. 3 that the $|S_{11}|$ is less than -10 dB for the entire analyzed frequency range of 1-6 THz for all antenna designs except with $h = 1 \mu\text{m}$. This reflects the ultra-wideband operational resonance characteristics of the designed Vivaldi antenna.

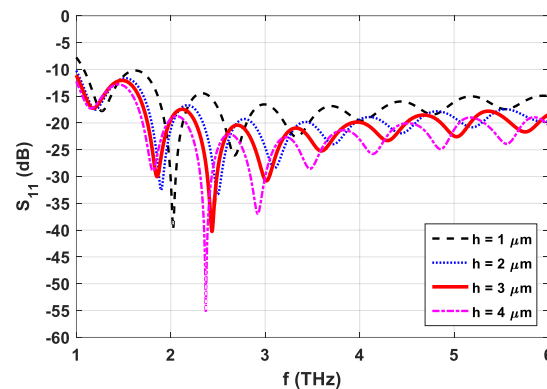


Fig. 3. Effect of substrate thickness (h) on the reflection parameter.

The variations in the reflection characteristics of the proposed antenna with the change in the thickness of the used conducted material as Vivaldi patch are illustrated in Fig. 4. We observe that the resonance properties of the antenna improve with the enhancement of the -10 dB impedance bandwidth (for $|S_{11}| < -10$ dB) with the increase in the gold thickness from 0.04 μm to 0.07 μm . Figures 5 and 6 depict the comparison of the S_{11} characteristics of the antenna for the different values of the length (L_G) and width (W_G) of the Vivaldi patch of Fig. 1. The length and width of the gold conductor Vivaldi patch are varied from 110 μm to 125 μm and 18 μm to 24 μm , respectively. The results of Figs. 5 and 6 deduces that the variations of the length and width of the gold conductor material in the aforementioned ranges did not bring a significant change in the reflection properties of the designed Vivaldi antenna.

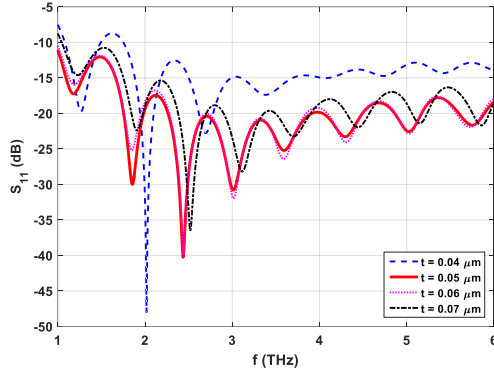


Fig. 4. Effect of Vivaldi patch thickness (t) on the reflection parameter.

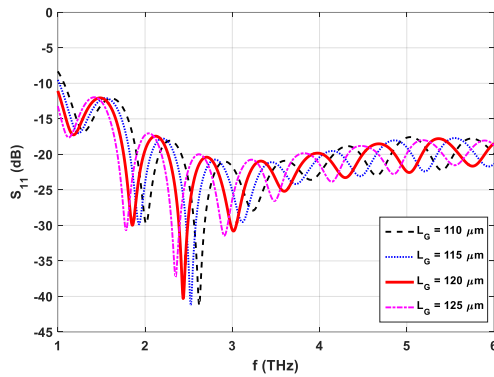


Fig. 5. Effect of length of Vivaldi patch (L_G) on the reflection parameter.

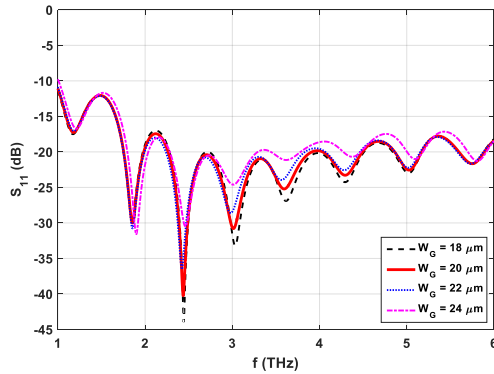


Fig. 6. Effect of Vivaldi patch width (W_G) on the reflection parameter.

Figure 7 reflects the changes in the reflection characteristics of the Fig. 1 antenna when the value of the slot curvature exponential variable (a) varies from $0.5 \mu\text{m}$ to $0.8 \mu\text{m}$. As expected, the results depict that the exponential variable is the critical design parameters of the antenna as its variations have significant impact on the resonance properties of the antenna. As like the slot

curvature variations, the change in the minimum width of the slot (g) also have adverse impact on the reflection parameters of the designed THz antenna (see Fig. 8). The results of Fig. 8 shows that among the varied range of g , *i.e.*, $0.1 \mu\text{m}$ to $0.4 \mu\text{m}$, the best resonance characteristics are observed for the lowest value in the range, *i.e.*, $0.1 \mu\text{m}$.

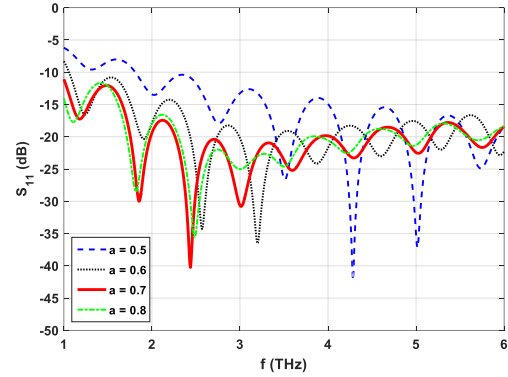


Fig. 7. Effect of slot curvature exponential variable (a) on the reflection parameter.

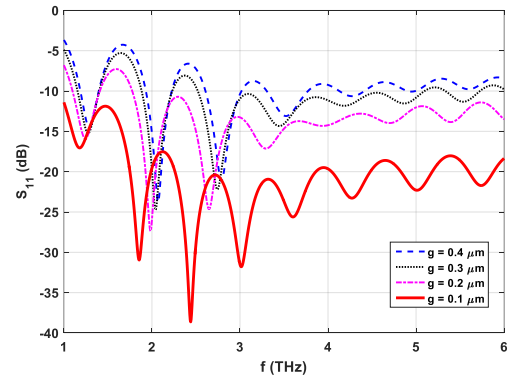


Fig. 8. Effect of slot minimum width (g) on the reflection parameter.

We noted from the comparison of the Figs. 3-8 results that for the designed Vivaldi THz PCA the critical design parameters are the thickness of used antenna substrate and conductive patch, exponential curvature and minimum thickness of the antenna slot as the variations of these parameters significantly impact the wideband resonance characteristics and -10 dB impedance bandwidth of the antenna. The parameter analysis of antenna design variables (Figs. 3-8) deduces that the optimal values of the designed Vivaldi antenna for the UWB resonance characteristics are $L_S = 134 \mu\text{m}$, $W_S = 60 \mu\text{m}$, $h = 3 \mu\text{m}$, $t = 0.05 \mu\text{m}$, $L_G = 120 \mu\text{m}$, $W_G = 20 \mu\text{m}$, $a = 0.7 \mu\text{m}$, and $g = 0.1 \mu\text{m}$. The red color waveforms in Figs. 3-8 represents the aforementioned optimal design parameters results of the Fig. 1 antenna without lens.

IV. OPTIMIZED UWB THz VIVALDI ANTENNA WITHOUT LENS

After obtained the optimized parameters of the Fig. 1 antenna design with the impedance matching, the performance of the optimized antenna is analyzed in terms of its radiation characteristics and axial ratio.

Figure 9 shows the optimized results of the reflection coefficient of the designed THz PCA antenna. The directivity results of the optimized Vivaldi antenna without lens are depicted in Fig. 10. We can note that the antenna has almost greater than 5 dBi directivity values from 3 to 6 THz range. The maximum observed values of the directivity of the designed optimized antenna is 6.8 dBi without the added lens. As like the directivity results, it can be observed from the Figs. 11 – 13 results that the optimized design antenna exhibits higher values of the gain, total efficiency and radiation efficiency of the antenna in the frequency band of 3 to 6 THz. The total efficiency and radiation efficiency of the antenna increases with the increase in the frequency till 3 THz and each has maximum value of 16% in the analyzed frequency band of 1 to 6 THz (see Figs. 12 and 13). The optimized antenna exhibits > 10% total and radiation efficiency values from 2 THz onward. Figure 14 depicts the axial ratio results of the optimized THz Vivaldi antenna. The results illustrate that designed antenna has excellent axial ratio bandwidth of 6 THz similar to its 6 THz -10 dB impedance bandwidth. The reported results of 6 THz ultra-wideband impedance and axial ratio bandwidths are not reported in literature [1, 10, 13, 14, 16-19, 27, 28] to be the best of our knowledge.

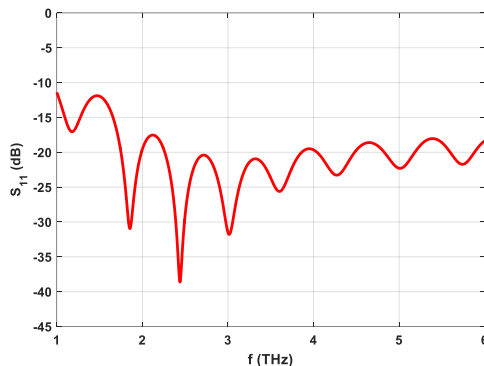


Fig. 9. Reflection coefficient of the optimized THz antenna without lens.

Figure 15 presents the far-field 3D radiation patterns of the optimized antenna at four different frequencies of 1.85 THz, 2.45 THz, 3.6 THz and 5 THz respectively. We note that the directivity of the designed antenna increases with the increase of the frequency. The observed maximum values of directivities at 1.85 THz, 2.45 THz,

3.6 THz and 5 THz are 3.38 dBi, 3.59 dBi, 6.71 dBi and 5.31 dBi respectively. The current distribution results of the designed Vivaldi antenna are shown in Fig. 16. The levels of the distributed current around the antenna taper reduces with the increase in the frequency which increases the directivity of the antennas as depicted in the Fig. 15 radiation pattern results.

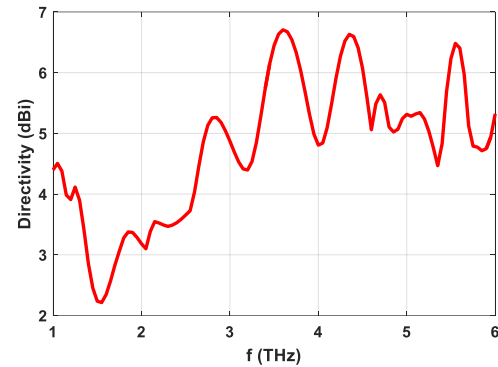


Fig. 10. Directivity of the optimized THz antenna without lens.

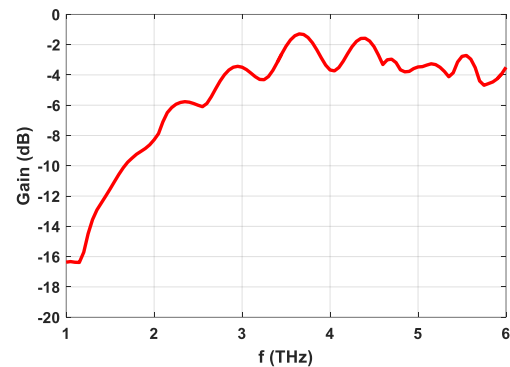


Fig. 11. Gain of the optimized THz antenna without lens.

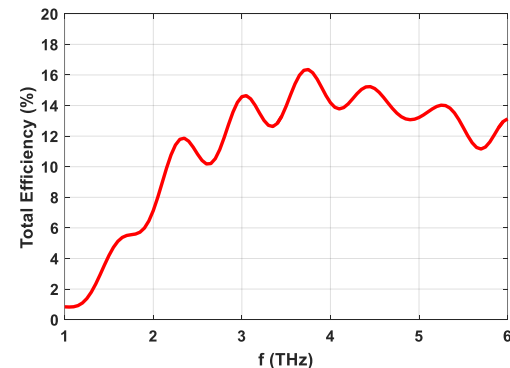


Fig. 12. Total efficiency of the optimized THz antenna without lens.

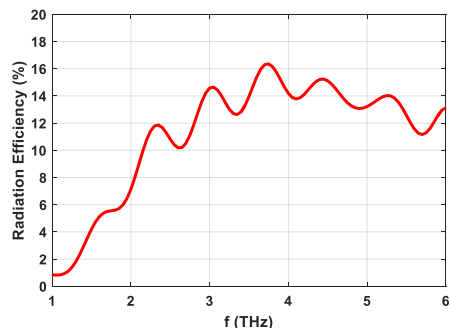


Fig. 13. Radiation efficiency of the optimized THz antenna without lens.

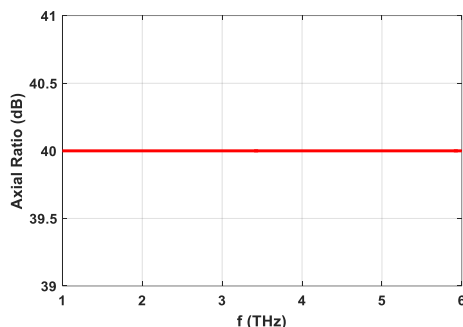


Fig. 14. Axial ratio of the optimized THz antenna without lens.

V. DESIGNED OPTIMIZED VIVALDI ANTENNA WITH LENS

The purpose of adding the lens in the antenna structure was to enhance its radiation characteristics. The analysis of the parametric variations in the diameter (R_L) of the added lens in the antenna structure (see Fig. 2) is performed with the obtained optimized other antenna design parameters from Section III. The diameter of the lens is varied in the range of $65 \mu\text{m}$ to $105 \mu\text{m}$ with a step size of $20 \mu\text{m}$.

Figure 17 shows the variations in the impedance bandwidth of the Fig. 2 antenna for the three different values of the integrated lens diameter. We observed that with all three analyzed values of lens diameter, the antenna exhibits UWB resonance characteristic in the

complete analyzed THz frequency range of 1 to 6 THz. The comparison of the Fig. 9 and 17 S_{11} results shows that the resonance frequencies of the antenna changes with the addition of the hemispherical lens in the antenna structure. However, the 6 THz impedance bandwidth of the antenna did not change as the reflection coefficient characteristics remains less than -10 dB in the entire analyzed frequency band.

Figure 18 illustrates the change in the directivity of the THz antenna with the change in lens diameter while the variations in the total efficiency of the designed antenna with the change in lens diameter are depicted in Fig. 19. Figure 18 shows that overall directivity of the designed antenna increases with the increase in the diameters of the lens due to the localization of the current distribution around the source of the antenna with the addition of large diameter lens. However, the change in lens diameter have minimal effect on the total efficiency of the antenna as depicted in Fig. 19 waveforms. As expected, the directivity and total efficiency of the antenna has been increased by around 40-50% with the addition of the lens in the antenna structure due to the enhanced optical-to-terahertz coupling.

Figure 20 shows the axial ratio of the optimized antenna with the change in the lens diameters. The AR characteristics of the antenna did not change with the variations in the lens diameters as like impedance matching, directivity and total efficiency of the antenna. Figure 20 only shows one waveform which depicts the AR results of all three cases of change in lens diameter, *i.e.*, $65 \mu\text{m}$, $85 \mu\text{m}$ and $105 \mu\text{m}$. The AR bandwidth is defined in terms of the frequency range for which $\text{AR} > = 3 \text{ dB}$. The results show that AR bandwidth of the designed antenna covers the total analyzed frequency range, *i.e.*, 1-6 THz which results in 3-dB AR bandwidth of 6 THz for the optimized THz Vivaldi antenna. The comparison of the AR results of the antenna with (Fig. 20) and without lens (Fig. 14) deduces that the AR characteristics of the reported Vivaldi antenna did not change with and without the lens on the antenna structure. The comparison of the Figs. 17 to 20 show that the more better performance of the antenna in terms of resonance, directivity and total efficiency of the antenna are obtained when the diameter of the lens is increased, *i.e.*, for the antenna lens of $105 \mu\text{m}$.

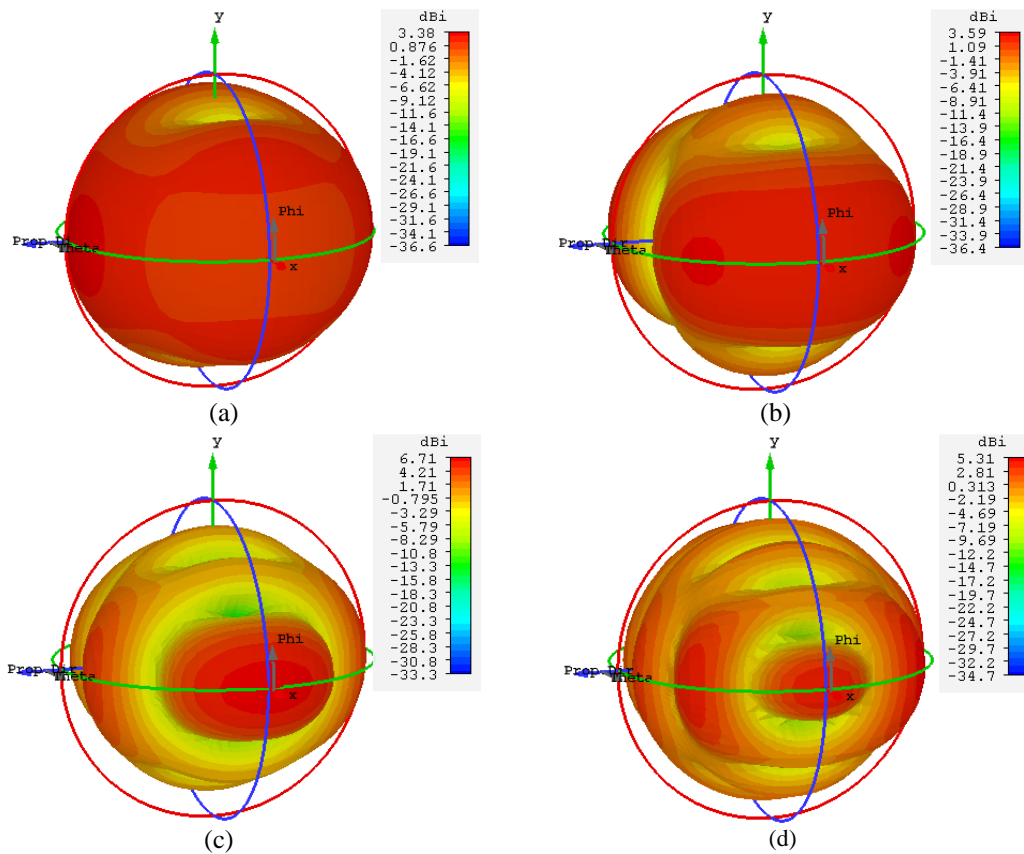


Fig. 15. Far field 3-D radiation patterns of optimized antenna without a lens for different frequencies: (a) 1.85 THz, (b) 2.45 THz, (c) 3.6 THz, and (d) 5 THz.

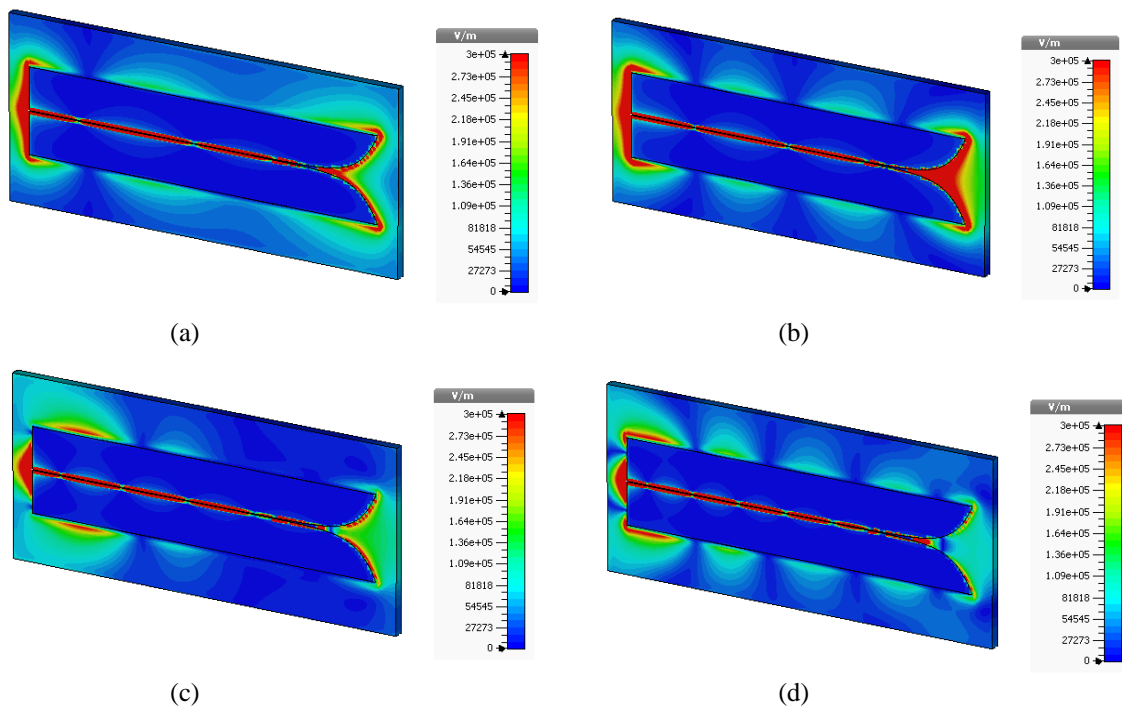


Fig. 16. Comparison of current distribution of optimized antenna without a lens for different frequencies: (a) 1.85 THz, (b) 2.45 THz, (c) 3.6 THz, and (d) 5 THz.

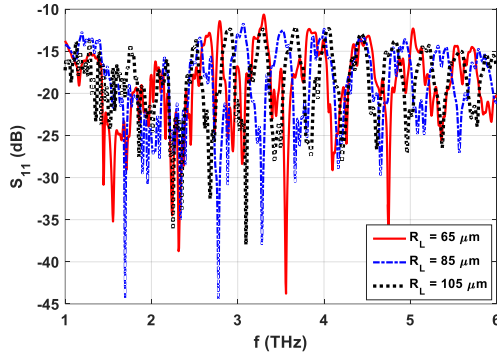


Fig. 17. Effect of lens diameter (R_L) on the reflection parameters of the optimized antenna.

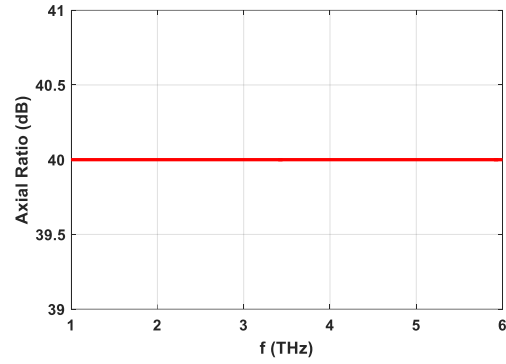


Fig. 20. Effect of lens diameter (R_L) on the axial ratio of the optimized antenna.

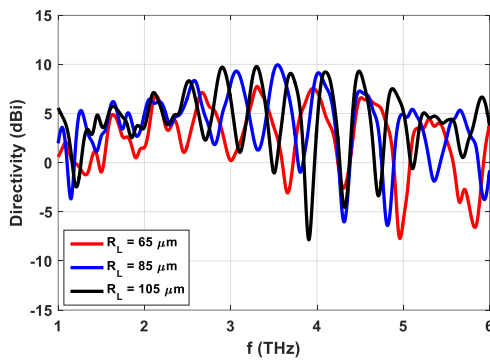


Fig. 18. Effect of lens diameter (R_L) on the directivity of the optimized antenna.

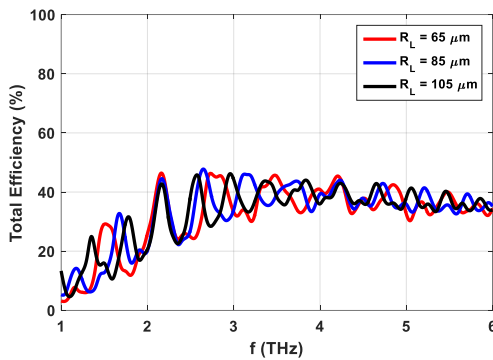


Fig. 19. Effect of lens diameter (R_L) on the total efficiency of the optimized antenna.

Figure 21 presents the comparison of the far field radiation patterns of the optimized Vivaldi antenna with three different values of integrated lens diameter. The far field results of Fig. 20 are for the four resonance frequencies of each design. The observed values of maximum gain for the 65 μm diameter design are 8.37 dBi, 7.05 dBi, 10.2 dBi and 12.6 dBi at the resonance frequencies of 1.95 THz, 2.45 THz, 3.35 THz and 5.1 THz, respectively. The change in the maximum gain for the antenna having lens with diameter of 85 μm is as follows: 6.75 dBi @ 1.5 THz, 9.93 dBi @ 3 THz, 11.6 dBi @ 3.6 THz and 14.8 dBi @ 5.4 THz. The last analyzed antenna design was of 105 μm for which the observed maximum gain values are 6.62 dBi, 11.4 dBi, 12.2 dBi and 13.1 dBi at the analyzed resonance frequencies of 1.55 THz, 2.9 THz, 3.7 THz and 4.4 THz respectively. This comparison reflects that overall the gain of the antennas increases with the increase in the frequency for all three designs of 65 μm , 85 μm and 105 μm respectively.

The comparison of the change in the directive and radiation characteristics of the antenna with a without lens is depicted in Fig. 22 for the antenna with lens meter of 65 μm . The graphical results of the other two designs of 85 μm and 105 μm are similar which are not reported here for brevity. The results of Fig. 22 illustrate that the side-lobe levels of the antenna decreases with the addition of the lens in the antenna structure as shown in Fig. 2. It makes the antenna more directive as can be noted from the results of Fig. 22.

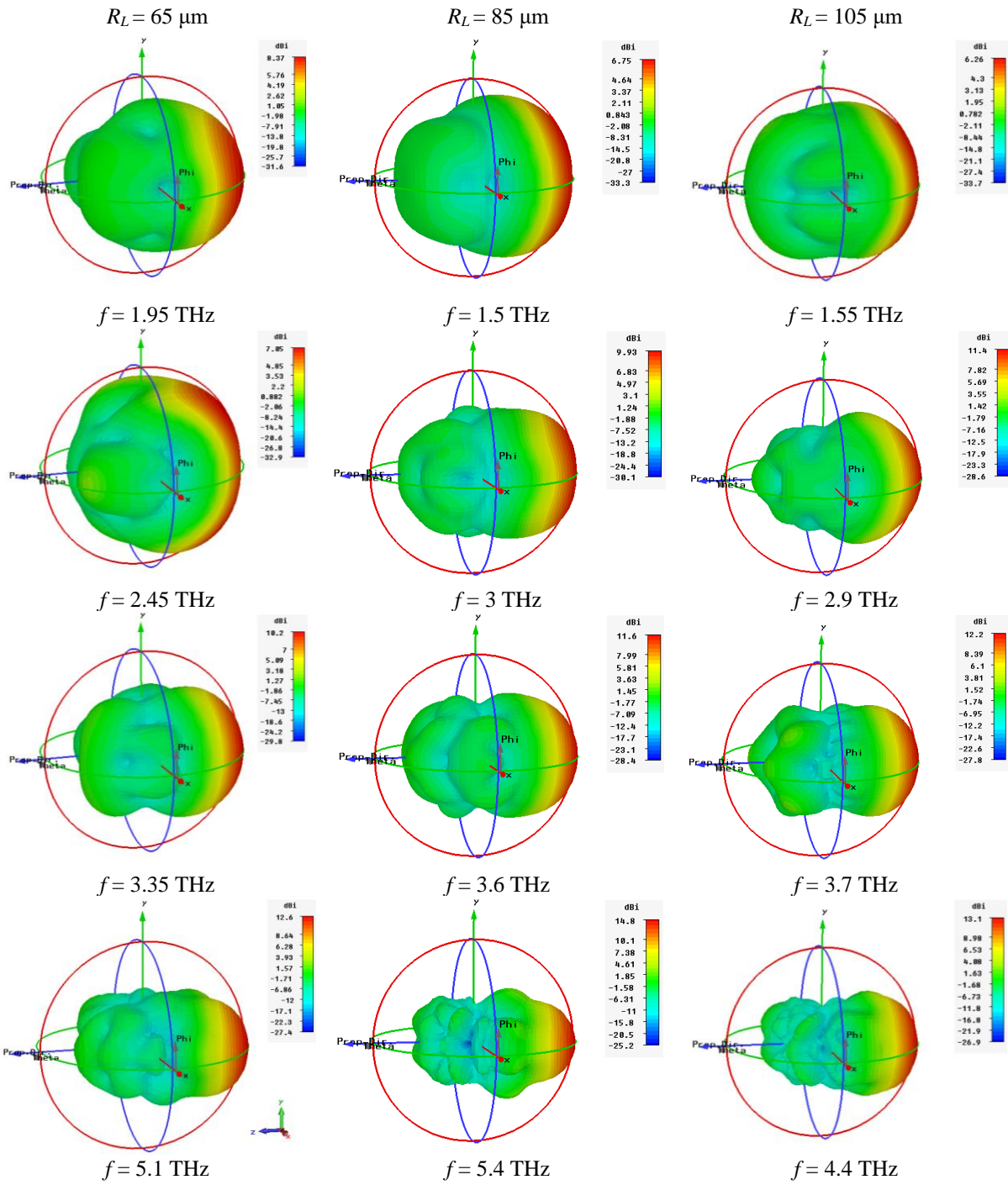


Fig. 21. Comparison of far-field radiation patterns of optimized antenna with different lens diameters.

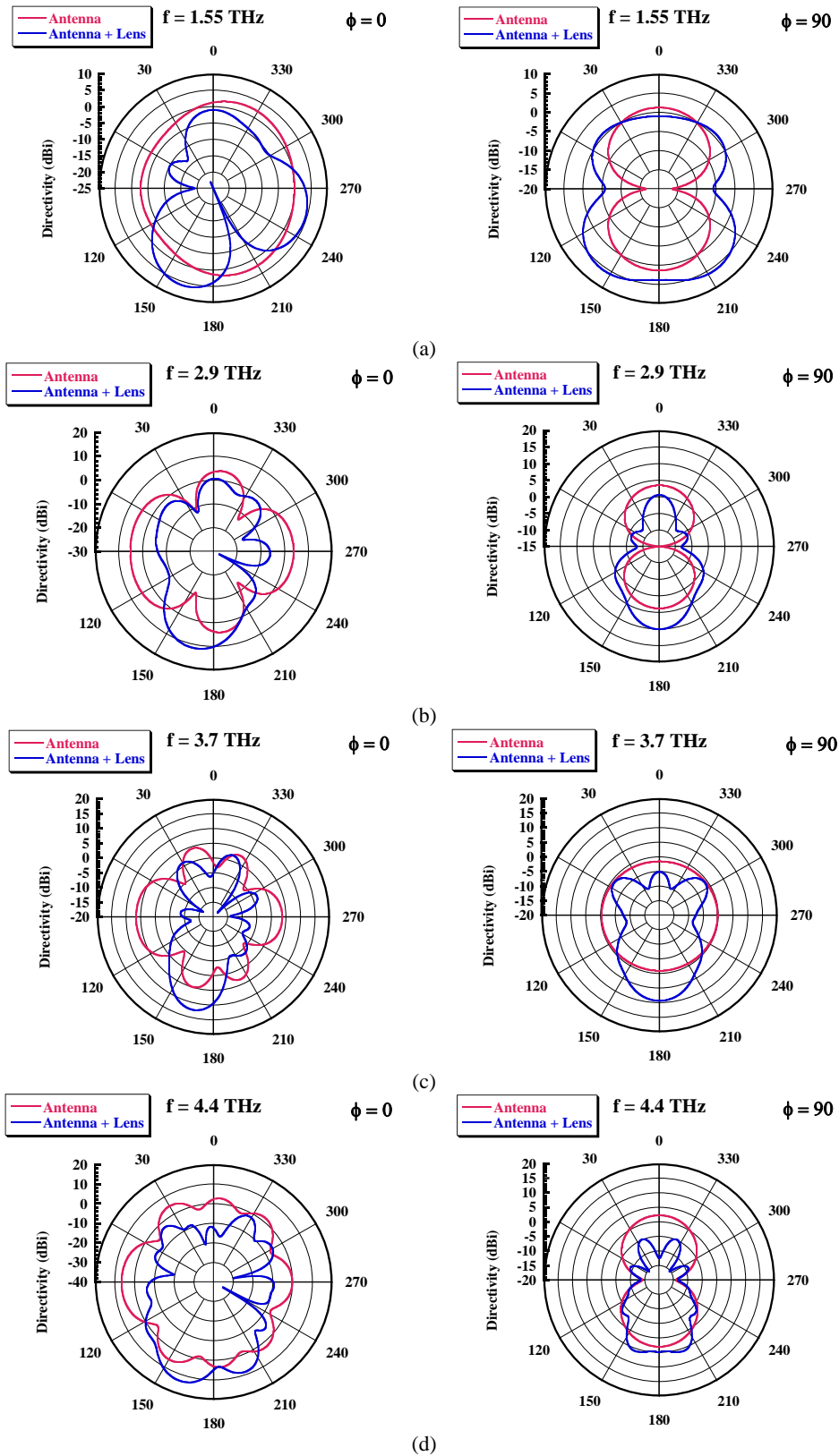


Fig. 22. Comparison of radiation patterns of optimized antenna with and without a lens for different frequencies at $\phi = 0^\circ$ and 90° : (a) 1.55 THz, (b) 2.9 THz, (c) 3.7 THz, and (d) 4.4 THz.

Table 2: Comparison of half power beamwidth (HPBW) of proposed UWB Vivaldi PCA

Frequencies	HPBW @ $\phi = 0^\circ$		HPBW @ $\phi = 90^\circ$	
	Without Lens	With Lens	Without Lens	With Lens
$f = 1.55$ THz	-	43°	84°	123°
$f = 2.9$ THz	94°	45°	78°	36°
$f = 3.7$ THz	64°	33°	-	34°
$f = 4.4$ THz	46°	39°	74°	60°

Table 3: Comparison of proposed UWB Vivaldi PCA design with the legacy design

References	Antenna Type	Substrate	Antenna Electrode Material	Lens	-10 dB Impedance Bandwidth (THz)	Maximum Directivity (dBi)	3dB AR Bandwidth (THz)
[14]	Bow-tie PCA with lens	GaAs	TiAu /AuGe / AuCr	Si hemispherical lens	0.20	10.85	-
[17]	Dipole planner array with FSS	LT-GaAs	Ti-Au	FSS	0.37	13.2	-
[13]	Bow-tie PCA with lens and dielectric coating	SI-GaAs	AuGe	HRFZ-Si lens	-	-	-
[1]	Bow-tie PCA without lens	LT-GaAs	Ti-Au	No lens	0.18	8.0	-
	Bow-tie PCA with lens			Si hemispherical lens		11.8	
	Bow-tie PCA with lens and combined with metasurface superstrate			No lens		11.9	
[18]	Yagi-Uda	GaAs	Ti-Au	No lens	0.02	10.9	-
[19]	Spiral-shaped	Si	Al	No lens	0.25	-	-
[28]	Dipole-type PCA with lens	GaAs	Gold	Aspheric lens	0.80	-	-
[10]	Conical horn	GaAs	-	Si-lens	-	18.5	-
[16]	Nanoplasmonic bow-tie PCA	GaAs	Cr/Au	No lens	1.00	-	-
Proposed Work	Vivaldi	Quartz	Gold	No lens	6.00	6.8	6.00
				Si hemispherical lens	6.00	10	6.00

Table 2 presents the comparison of the half power beamwidth (HPBW) of the designed UWB Vivaldi PCA for different analyzed frequencies of Fig. 22. It can be noted that the addition of the lens reduces the HPBW of the antenna in both azimuth and elevation planes. This increases the directivity of the antenna as can be seen in the radiation pattern results of Fig. 22.

VI. COMPARISON WITH LEGACY DESIGNS

The comparison of the proposed Vivaldi PCA antenna with the different reported PCA designs is summarized in Table 3. The comparison reflects that the presented THz PCA have the maximum impedance and AR bandwidth of 6 THz among all the legacy designs [1, 10, 13, 14, 16-19, 28]. Some of the reported PCA have higher directivity characteristics than the presented design, however the performance of proposed design remains superior in terms of impedance bandwidth and AR characteristics.

VII. CONCLUSION

The study has reported a novel design of the THz Vivaldi photoconductive antenna which has ultra-wideband impedance and AR bandwidths of 6 THz. The design of the proposed antenna was optimized using a detailed parametric study. The study includes the detailed analysis of the enhancement of the directivity and total efficiency (up to 40-50%) of the antenna with the addition of hemispherical based silicon lens. The presented design is first of its kind and has the potential to be used in the THz imaging and sensing applications as the powerful wideband and polarization insensitive THz source.

ACKNOWLEDGMENT

The project was funded by the Deanship of Scientific Research (DSR), King Abdulaziz University, Jeddah, Saudi Arabia under Grant No. KEP-23-135-38. The authors, therefore, acknowledge with thanks DSR technical and financial support.

REFERENCES

- [1] N. Zhu and R. W. Ziolkowski, "Photoconductive THz antenna designs with high radiation efficiency, high directivity, and high aperture efficiency," *IEEE Transactions on Terahertz Science and Technology*, vol. 3, no. 6, pp. 721-730, 2013.
- [2] P. U. Jepsen, D. G. Cooke, and M. Koch, "Terahertz spectroscopy and imaging – Modern techniques and applications," *Laser & Photonics Reviews*, vol. 5, no. 1, pp. 124-166, Jan. 2011.
- [3] I. Kasalynas, R. Venckevicius, and G. Valusis, "Continuous wave spectroscopic terahertz imaging with InGaAs bow-tie diodes at room temperature," *IEEE Sensors Journal*, vol. 13, no. 1, pp. 50-54, 2013.
- [4] Y. C. Shen, T. Lo, P. F. Taday, B. E. Cole, W. R. Tribe, and M. C. Kemp, "Detection and identification of explosives using terahertz pulsed spectroscopic imaging," *Applied Physics Letters*, vol. 86, no. 24, p. 241116, June 2005.
- [5] G. Rana, A. Bhattacharya, A. Gupta, D Ghindani, R. Jain, S. P. Duttagupta, and S. S. Prabhu, "A polarization-resolved study of nanopatterned photoconductive antenna for enhanced terahertz emission," *IEEE Transactions on Terahertz Science and Technology*, vol. 9, no. 2, pp. 193-199, 2019.
- [6] B. M. Fischer, M. Walther, and P. U. Jepsen, "Far-infrared vibrational modes of DNA components studied by terahertz time-domain spectroscopy," *Physics in Medicine and Biology*, vol. 47, no. 21, pp. 3807-3814, Oct. 2002.
- [7] K. Serita, S. Mizuno, H. Murakami, I. Kawayama, Y. Takahashi, M. Yoshimura, Y. Mori, J. Darmo, and M. Tonouchi, "Scanning laser terahertz near-field imaging system," *Optics Express*, vol. 20, no. 12, pp. 12959-12965, June 2012.
- [8] S. Yu, B. J. Drouin, and J. C. Pearson, "Terahertz spectroscopy of the bending vibrations of acetylene 12C2H2," *The Astrophysical Journal*, vol. 705, no. 1, pp. 786-790, Oct. 2009.
- [9] W. Zhang, A. K. Azad, and D. Grischkowsky, "Terahertz studies of carrier dynamics and dielectric response of n-type, freestanding epitaxial GaN," *Applied Physics Letters*, vol. 82, no. 17, pp. 2841-2843, Apr. 2003.
- [10] U. Deva and C. Saha, "Gain enhancement of photoconductive THz antenna using conical GaAs horn and Si lens," in *2016 International Symposium on Antennas and Propagation (APSYM)*, pp. 1-3, 2016.
- [11] A. Dhiflaoui, A. Yahyaoui, J. Yousaf, S. Bashir, B. Hakim, T. Aguilu, H. Rmili, and R. Mitra, "Numerical analysis of wideband and high directive bowtie THz photoconductive antenna," *Applied Computational Electromagnetic Society (ACES) Journal*, vol. 35, no. 6, pp. 662-672, June 2020.
- [12] I. A. Glinskiy, R. A. Khabibullin, and D. S. Ponomarev, "Total efficiency of the optical-to-terahertz conversion in photoconductive antennas based on LT-GaAs and In_{0.38}Ga_{0.62}As," *Russian Microelectronics*, vol. 46, no. 6, pp. 408-413, Nov. 2017.
- [13] A. Gupta, G. Rana, A. Bhattacharya, A. Singh, R. Jain, R. D. Bapat, S. P. Duttagupta, and S. S. Prabhu, "Enhanced optical-to-THz conversion efficiency of photoconductive antenna using dielectric nano-layer encapsulation," *APL Photonics*, vol. 3, no. 5, p. 051706, May 2018.
- [14] A. Jyothi, C. Saha, B. Ghosh, R. Kini, and C. Vaisakh, "Design of a gain enhanced THz bow-tie photoconductive antenna," in *2016 International Symposium on Antennas and Propagation (APSYM)*, pp. 1-3, 2016.
- [15] A. Dhiflaoui, A. Yahyaoui, J. Yousaf, T. Aguilu, B. Hakim, H. Rmili, and R. Mitra, "Full wave numerical analysis of wideband and high directive log spiral THz photoconductive antenna," *International Journal of Numerical Modelling: Electronic Networks, Devices and Fields*, vol. n/a, no. n/a, p. e2761.
- [16] S.-G. Park, Y. Choi, Y.-J. Oh, and K.-H. Jeong, "Terahertz photoconductive antenna with metal nanoislands," *Optics Express*, vol. 20, no. 23, pp. 25530-25535, Nov. 2012.
- [17] I. Malhotra, K. R. Jha, and G. Singh, "Design of highly directive lens-less photoconductive dipole antenna array with frequency selective surface for terahertz imaging applications," *Optik*, vol. 173, pp. 206-219, Nov. 2018.
- [18] K. Han, Y. Park, S. Kim, H. Han, I. Park, and H. Lim, "A terahertz Yagi-Uda antenna for high input impedance," in *2008 33rd International Conference on Infrared, Millimeter and Terahertz Waves*, pp. 1-2, 2008.
- [19] R. Singh, C. Rockstuhl, C. Menzel, T. P. Meyrath, M. He, H. Giessen, F. Lederer, and W. Zhang, "Spiral-type terahertz antennas and the manifestation of the Mushlake principle," *Optics Express*, vol. 17, no. 12, pp. 9971-9980, June 2009.
- [20] F. Sizov, O. Golenkov, I. Lysiuk, and A. Shevchik-Sheker, "THz and IR detectors in applications," in *2019 IEEE 8th International Conference on Advanced Optoelectronics and Lasers (CAOL)*, pp. 40-45, 2019.
- [21] C. Dong, W. Shi, F. Xue, and Y. Hang, "Multi-energy valley scattering characteristics for a SI-GaAs-based terahertz photoconductive antenna in linear mode," *Applied Sciences*, vol. 10, no. 1, p. 7, 2020.
- [22] M. Tani, S. Matsuura, K. Sakai, and S.-I. Nakashima, "Emission characteristics of photoconductive antennas based on low-temperature-grown GaAs

- and semi-insulating GaAs," *Applied Optics*, vol. 36, no. 30, pp. 7853-7859, Oct. 1997.
- [23] N. M. Burford and M. O. El-Shenawee, *Review of Terahertz Photoconductive Antenna Technology*, (J. Optical Engineering) SPIE, pp. 1-20, 2017.
- [24] L. Hou and W. Shi, "An LT-GaAs terahertz photoconductive antenna with high emission power, low noise, and good stability," *IEEE Transactions on Electron Devices*, vol. 60, no. 5, pp. 1619-1624, 2013.
- [25] A. Jooshesh, F. Fesharaki, V. Bahrami-Yekta, M. Mahtav, T. Tiedje, T. E. Darcie, and R. Gordon, "Plasmon-enhanced LT-GaAs/AlAs heterostructure photoconductive antennas for sub-bandgap terahertz generation," *Optics Express*, vol. 25, no. 18, pp. 22140-22148, Sep. 2017.
- [26] M. S. Kong, J. S. Kim, S. P. Han, N. Kim, K. Moon, K. H. Park, and M. Y. Jeon, "Terahertz radiation using log-spiral-based low-temperature-grown InGaAs photoconductive antenna pumped by mode-locked Yb-doped fiber laser," *Optics Express*, vol. 24, no. 7, pp. 7037-7045, Apr. 2016.
- [27] Q. Yu, J. Gu, Q. Yang, Y. Zhang, Y. Li, Z. Tian, C. Ouyang, J. Han, J. F. O'Hara, and W. Zhang, "All-dielectric meta-lens designed for photoconductive terahertz antennas," *IEEE Photonics Journal*, vol. 9, no. 4, pp. 1-9, 2017.
- [28] F. Formanek, M.-A. Brun, T. Umetsu, S. Omori, and A. Yasuda, "Aspheric silicon lenses for terahertz photoconductive antennas," *Applied Physics Letters*, vol. 94, no. 2, p. 021113, Jan. 2009.
- [29] P. J. Gibson, "The Vivaldi aerial," in *1979 9th European Microwave Conference*, pp. 101-105, 1979.